Reconfigurable Materials | Hot Paper

Selective Janus Particle Assembly at Tipping Points of Thermally-Switched Wetting**

Changqian Yu, Jie Zhang, and Steve Granick*

Abstract: *Thermal wetting can simply, selectively and reversibly join patchy particles into clusters (2D and 3D) and also colloidal crystals over the narrow temperature range of 1–2 °C. This is demonstrated with Janus particles (gold half-coated silica spheres) immersed in a binary mixture of water/2,6-lutidine, such that the relative strength of gold–gold bonding through hydrophobic interaction and silica–silica bonding through the wetting-induced attraction is reversibly switched according to temperature.*

The burgeoning interest in reconfigurable materials is a scientific challenge not achieved using conventional schemes of self-assembly.[1] Here we explore the approach of placing the system at a tipping point such that large changes in assembled structure are triggered by small, reversible environmental changes. If this could be achieved, it could be useful for potential applications that have been envisioned for reconfigurable colloids, for example adaptive optics and coatings.[2] Here, we describe our progress with a scheme that is easily generalized: the exquisitely sensitive temperature dependence of wetting in a suitable mixture of two fluids.

The scheme is summarized in Figure 1. Janus spheres (silica particles coated on one hemisphere with gold) are immersed in the mixture of water/2,6-lutidine, a binary fluid that has been widely studied to understand the physical chemistry of liquids[3] and recently to cause attraction between colloids whose surface chemistry is homogeneous.[4] We work with silica particles, for which the preferential wetting region (hatched region) lies below the phase transition temperatures of the binary liquid (gray region, Figure 1) and at lutidine compositions above its critical composition. The methods of Janus particle synthesis and in situ microscopic observation of them are described in the Supporting Information.

The opportunity to use this for reconfigurability comes because for Janus particles there are two pair interactions
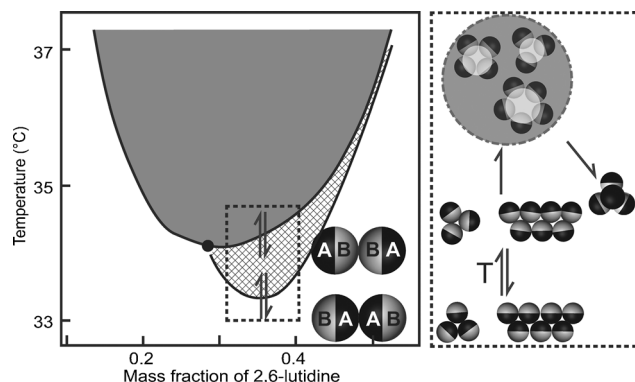

Figure 1. Scheme of switchable bonding between Janus particles in the context of the phase diagram of water/2,6-lutidine mixtures. In the left panel, A and B denote gold and silica hemispheres and arrows represent increasing and decreasing temperature. The top solid line shows the coexistence temperature of water/2,6-lutidine mixtures.[5] The bottom solid line is the preferential wetting temperature, estimated from when spheres first join in experiments, above which wetting causes silica surfaces to attract while the solvent mixture remains in one phase (hatched region between two lines). When the solvent mixture separates into two phases (gray region), particles segregate at interfaces of two-phase liquid mixture. The rectangle enveloped by dashed lines highlights the families of temperature and fluid composition studied here. The associated scheme of reversible particle assembly is described in the right panel.

whose relative dominance one can switch. Below the preferential wetting temperature, the charged silica surfaces repel one another while hydrophobicity of the gold-coated hemispheres (ζ potential of the gold surface ≈ 0 mV, Supporting Information) causes them to attract one another. But it is different at higher temperature: now, wetting forces from the preferential adsorption of water onto silica cause those hemispheres to attract (hatched region in Figure 1).[6] Such preferential water adsorption from the binary mixture also causes a right-shift[7] from the reported bulk critical point, which is mass fraction of 2,6-lutidine $x_L = 0.29$ and critical temperature $T_c = 34.0$ °C.[5] In experiments reported below, the mass fraction was chosen slightly off-critical, $x_L = 0.35$, to encourage wetting, unless noted otherwise. At this composition, bulk demixing occurs at 34.2 °C and the preferential wetting temperature is 0.8 to 1.0 °C lower than this. As preferential wetting shifts the coexistence curve to higher lutidine fraction, this temperature window is larger than that at the critical composition quantified previously by total internal reflection microscopy.[4a] At even higher temperatures, one enters a zone of macroscopic phase separation in which Janus particles assemble as Pickering emulsions at the

[*] C. Yu, J. Zhang, Prof. S. Granick
Department of Materials Science and Engineering
University of Illinois
Urbana, IL 61801 (USA)
E-mail: sgranick@illinois.edu
Homepage: http://groups.mrl.uiuc.edu/granick/
Prof. S. Granick
Department of Chemistry, and Department of Physics
Urbana, IL 61801 (USA)

interfaces[8] between the two phases, as shown in Figure S1, except that this association is reversible unlike conventional Pickering emulsions. This unusual property opens the door to assemble conveniently both 3D clusters and 2D crystals.

After particles sediment onto planar silica substrates, assembly is confined to be planar as for the 3 µm spheres that we consider, the single-particle gravitational height of ca. 25 nm[9] is much less than the particle diameter. There are two extremes to consider. Below the wetting temperature and when local particle concentration is low ($\phi = 0.3$ to 0.5), we observe small clusters (dimers and trimers mostly; Figure 2a)
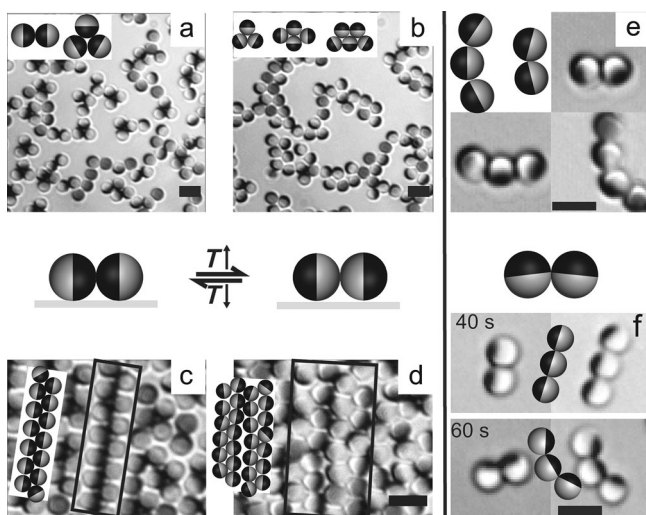

Figure 2. Reconfigurable assembly of 2D Janus particle clusters through switchable bonding. a) Gold–gold bonded clusters. b) Silica–silica clusters bonded by preferential wetting. c) Gold–gold bonded zigzag chain. d) Chain unzipped by silica–silica bonding. e) Angled chains joined by side-by-side bonding. f) The dependence of chain curvature on gold etching time of 40 s (top) and 60 s (bottom). To actuate this reconfiguration by switching on and off the silica–silica attraction, we employ temperature changes between 1.0°C and 0.2°C below the demixing temperature, which is 34.2°C at $x_L = 0.35$. Scale bars are 5 µm.

joined by hydrophobicity of the gold coating but with attraction so weak that the particles rotate even when gold patches are located close together (Movie S1). But above the preferential wetting temperature, the water-rich phase accumulates at silica, leading to silica-bonded clusters (Figure 2b and Movie S1). Closely dense-packed 2D colloids (local $\phi = 0.7$–0.8) produce extended planar structures, gold-bonded zigzag chains below the wetting temperature, highlighted in Figure 2c, with persistent shape that vibrates thermally (Movie S2). Upon further increase of temperature, silica–silica attraction "unzips" these chains, resulting in silica–silica bonded long chain aggregates (Figure 2d and Movie S2) in which the strong wetting force quenches particle vibrations. Bond switching occurs generally, regardless of the local particle concentration. For example, in Figure S2 one can notice that trimers are the most abundant state, yet the fraction of zigzag chains increases as the concentration

approaches the close-packed regime, mainly due to higher effective pressure contributed by neighbouring particles.[10] Note that this spectrum of self-assembled structures is controlled by small changes of temperature, 1–2°C, and requires no chemical modification. During multiple temperature cycles, joining and disjoining of silica–silica bonds occurs within < 1 s around 1.0°C below the demixing temperature, provided the composition is at the relatively low value $x_L = 0.35$. When the lutidine fraction is higher, $x_L > 0.40$, hysteresis is prominent. For example, silica-joined clusters are seen to persist even > 1.0°C below the preferential wetting temperature.

It may at first seem odd that Janus particles line up parallel to their equators but this is what we observed and it confirms a prediction from computer simulations for a slightly different physical system.[11] Joined at their silica–gold boundaries rather than face-to-face (Figure 2e) above the preferential wetting temperature, in the present system it seems that this configuration minimizes electrostatic repulsion while retaining wetting attraction. Physically, the probable reason is that wetting-induced attraction extends over more than a hemisphere area, because directional vacuum-phase gold deposition in the synthesis step (Supporting Information) meets the spheres from above, producing negligibly small thickness near the equator. To test this interpretation, we lessened the size of the attractive patch by etching away the edge of the gold coating. This caused the chains to bend towards the gold sides. It is analogous to what happens with small-molecule surfactants, where changing the head-to-tail ratio (the HLB balance) likewise causes curvature change in surfactant assemblies.[12] Examples of HLB balance in the present system are shown in Figure 2e and f. Relatively large gold patches cause chains to bend with their silica patch inward; relatively small gold patches cause chains to bend with their silica patch facing outward.

This assembly method is not restricted to forming planar structures. To form clusters, we adapt the pioneering droplet shrinkage method of Pine and co-workers,[13] but exploiting the unique reversibility of the present system. Demonstrating the idea, we worked at mass fraction $x_L \approx 0.50$, which is above the critical concentration. The scheme with temperature cycles is shown in Figure 3a. Raising temperature to 0.5–1.0°C above the phase separation temperature produces a water-in-oil emulsion within which multiple Janus particles accumulate. Upon cooling to the miscible state, particles within shrinking water droplets organize into well-ordered clusters, the source of attraction being capillary forces from water-rich menisci between silica hemispheres. These clusters are stable for hours up to 5°C below the phase separation temperature at this lutidine composition, because water menisci persist due to wetting hysteresis.[14] Figure 3b and Movie S3 illustrate a tetrahedron formed this way. Note that the cluster size is determined by the number of particles trapped, and that the larger clusters usually form from coalescence of small droplets. Figure 3c shows additional larger clusters whose high symmetry is notable. Movie S4 further demonstrates reversibility: it shows the disassembly of a pyramid-shape pentamer upon deep cooling to 6°C below the phase separation temperature.
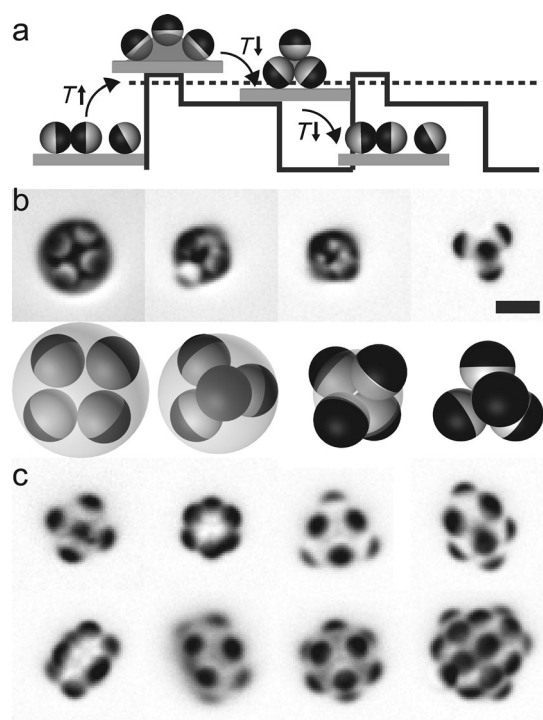
Figure 3. Formation of 3D clusters. a) Scheme of using temperature cycles to reversibly assemble 3D clusters. The dashed line is the bulk demixing temperature. Water-rich droplets are denoted in gray color. b) Data accompanied by schematic diagram showing that tetrahedra arise from droplet shrinkage. Temperature decreases from 0.5 °C above the demixing temperature (37.0 °C at $x_L = 0.50$) to 1.0 °C below that. From left to right, droplet size shrinks (gray). c) Representative images of 3D clusters with larger numbers of particles at 1.0 °C below the demixing temperature. The scale bar is 5 µm.

Figure 4. Assembly from particle–surface attraction. a) Particle orientation changes as temperature rises: state 1 (freely rotating particle at 33.2 °C), state 2 (gold–silica equator stands perpendicular to the substrate at 34.0 °C), state 3 (gold–silica boundary lies parallel to the substrate at 34.3 °C), state 4 (crystalline clusters of state 3 particles at 34.3 °C). States 4′ and 4″ are large crystals. The demixing temperature is 34.2 °C for $x_L = 0.35$. The scheme shows two steps of orientation flip upon temperature change. b) Coalescence-induced sudden collision of two particles and also multiple particles. The water-rich wetting layer droplets surrounding them are shown in gray circles imaged by defocusing the microscope slightly. Scale bars are 5 µm.

Another avenue to form droplets that subsequently shrink to form particle clusters exploits surface dewetting. To implement the idea, we designed the experiment such that water-rich droplets would dewet from a hydrophobic substrate. It was convenient to modify silica planar substrates with OTS monolayers (octadecyltrichlorosilane). The repulsive forces[4a] between OTS and silica hemispheres drives particles to develop structures with silica sides facing away from the substrate. When the particle concentration is small, usually $\phi < 0.3$, we observe small clusters similar to those in Figure 3. High particle concentration, usually $\phi > 0.5$, produces larger clusters, including micelles, tubes and even bilayers (Figure S3 and Movie S5). Note that while a computer simulation[15] has predicted bilayers and tube shapes to be unstable, the simulation prediction was for patches of equal area but as argued above, wetting-induced attraction can extend over an area larger than a hemisphere.

What if particles interact preferentially with the flat silica substrate? Beyond previously discussed switchable particle–particle bonding, particle–substrate interaction dominates as the particle density is kept low ($\phi < 0.10$). We observed orientational flips with increasing temperature (Figure 4a and Movie S6). Below the wetting temperature (stage 1), particles rotate freely out-of-plane with the gold hemisphere showing a preference for the substrate because of gravitational bias
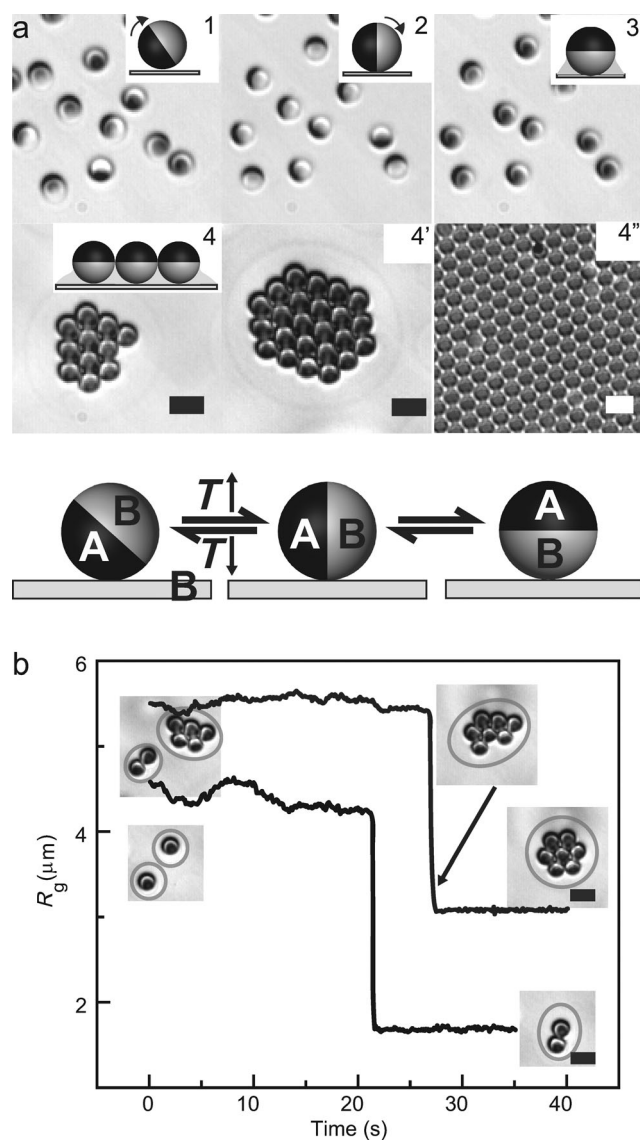
from the metal coating and electrostatic repulsion between silica and substrate. Within the preferential wetting regime (stage 2), particles align with their equators roughly perpendicular to the substrate, reflecting the compromise between gaining wetting force and minimizing silica-substrate repulsion and gravitational energy. Above the phase separation temperature, even just 0.1–0.3 °C above it (stage 3), water-rich droplets on the substrate trigger the particles to maximize contact of their silica hemispheres with the substrate.[16] This is so when the thickness of wetting droplets is less than the

particle radius such that the capillary attraction causes the particles to flip; the case of thicker wetting droplet is shown in Figure 3b. Of course, droplets tend to coalesce. Droplet coalescence causes particles to crystallize into perfect hexagonal packing (stage 4). Large crystals form rapidly from merger of droplet-coated regions of the substrate (stage 4′ and Movie S7) and even without droplet merger provided that the surface contains a high density of particles (stage 4″). To demonstrate thermal reversibility in this situation, crystals in stages 4′ and 4″ were gradually cooled to 1.5°C below the demixing temperature (Figure S4 and Movie S8). Interestingly, crystals of flipped particles, except those at edges, are found to survive even 0.6°C below the demixing temperature due to the residual water layers. Further decreasing temperature promotes complete dissolution of these water layers, leading the crystal to fall apart into individual particles and gold bonded zigzag chains, respectively, at these two concentrations.

This long-range "attractive" force causes swift particle–particle assembly at separations as large as tens of μm, illustrated in Movies S6 and S7. To confirm that the mechanism is coalescence between water-rich solvent droplets, we defocused the microscope to make the wetted regions visible, as drawn in the insets of Figure 4b. To quantify kinetics of the process, we computed the radii of gyration of these assemblies. Inspecting how this changes with time (Figure 4b), one identifies rapid (< 0.1 s) decrease of R_g and also rearrangements within the assemblies, illustrated by the arrow in Figure 4b.

We conclude by commenting on the generality and limitations of our approach. To make it work, it is necessary to have reversible switching of A–A and B–B bonding. Our system satisfies this criterion. But we found this approach fails when the hydrophobic attraction is too strong, specifically when C_{18}-thiol was used to make gold more hydrophobic, in which case particles became bound irreversibly (Figure S5). However, provided that reversibility is maintained, the approach appears to generalize nicely. We found that triblock particles coated with gold at the poles[17] similarly switch between gold–gold bonded dimers, trimers and chains (Figure S6). To exploit more complex patch arrangements and shape anisotropy[18] can be considered as a next step that follows logically. There exist other potentially effective approaches to achieve reconfigurable assemblies, especially use of DNA linkers,[19] but an advantage of this method is that there is no need to modify the surface chemically, provided that it is convenient to work under the solvent conditions of this experiment.

[1] a) Q. Chen, J. K. Whitmer, S. Jiang, S. C. Bae, E. Luijten, S. Granick, *Science* **2011**, *331*, 199–202; b) P. F. Damasceno, M. Engel, S. C. Glotzer, *Science* **2012**, *337*, 453–457; c) F. Li, D. P. Josephson, A. Stein, *Angew. Chem.* **2011**, *123*, 378–409; *Angew. Chem. Int. Ed.* **2011**, *50*, 360–388; d) H. Pei, L. Liang, G. Yao, J. Li, Q. Huang, C. Fan, *Angew. Chem.* **2012**, *124*, 9154–9158; *Angew. Chem. Int. Ed.* **2012**, *51*, 9020–9024; e) L. Phan, W. G. Walkup, D. D. Ordinario, E. Karshalev, J.-M. Jocson, A. M. Burke, A. A. Gorodetsky, *Adv. Mater.* **2013**, *25*, 5621–5625; f) J. S. Randhawa, T. G. Leong, N. Bassik, B. R. Benson, M. T. Jochmans, D. H. Gracias, *J. Am. Chem. Soc.* **2008**, *130*, 17238–17239; g) S. Sacanna, L. Rossi, D. J. Pine, *J. Am. Chem. Soc.* **2012**, *134*, 6112–6115; h) S. K. Y. Tang, R. Derda, A. D. Mazzeo, G. M. Whitesides, *Adv. Mater.* **2011**, *23*, 2413–2418.

[2] a) M. D. McConnell, M. J. Kraeutler, S. Yang, R. J. Composto, *Nano Lett.* **2010**, *10*, 603–609; b) O. D. Velev, E. W. Kaler, *Langmuir* **1999**, *15*, 3693–3698; c) Y. Zhang, F. Lu, D. van der Lelie, O. Gang, *Phys. Rev. Lett.* **2011**, *107*, 135701.

[3] a) M. Y. Lin, S. K. Sinha, J. M. Drake, X. L. Wu, P. Thiyagarajan, H. B. Stanley, *Phys. Rev. Lett.* **1994**, *72*, 2207–2210; b) D. W. Pohl, W. I. Goldburg, *Phys. Rev. Lett.* **1982**, *48*, 1111–1114.

[4] a) U. Nellen, L. Helden, C. Bechinger, *EPL* **2009**, *88*, 26001; b) F. Soyka, O. Zvyagolskaya, C. Hertlein, L. Helden, C. Bechinger, *Phys. Rev. Lett.* **2008**, *101*, 208301.

[5] C. A. Grattoni, R. A. Dawe, C. Y. Seah, J. D. Gray, *J. Chem. Eng. Data* **1993**, *38*, 516–519.

[6] a) B. M. Law, J. M. Petit, D. Beysens, *Phys. Rev. E* **1998**, *57*, 5782–5794; b) P. D. Gallagher, M. L. Kurnaz, J. V. Maher, *Phys. Rev. A* **1992**, *46*, 7750–7755.

[7] a) D. Beysens, T. Narayanan, *J. Stat. Phys.* **1999**, *95*, 997–1008; b) R. R. Netz, *Phys. Rev. Lett.* **1996**, *76*, 3646–3649.

[8] E. M. Herzig, K. A. White, A. B. Schofield, W. C. K. Poon, P. S. Clegg, *Nat. Mater.* **2007**, *6*, 966–971.

[9] V. Prasad, D. Semwogerere, E. R. Weeks, *J. Phys. Condens. Matter* **2007**, *19*, 113102.

[10] H. Shin, K. S. Schweizer, *Soft Matter* **2014**, *10*, 262–274.

[11] a) A. Giacometti, F. Lado, J. Largo, G. Pastore, F. Sciortino, *J. Chem. Phys.* **2010**, *132*, 174110; b) F. Sciortino, A. Giacometti, G. Pastore, *Phys. Rev. Lett.* **2009**, *103*, 237801.

[12] J. N. Israelachvili, *Intermolecular and Surface Forces*, revised 3rd ed., Academic Press, New York, **2011**, pp. 538–559.

[13] V. N. Manoharan, M. T. Elsesser, D. J. Pine, *Science* **2003**, *301*, 483–487.

[14] D. Bonn, H. Kellay, G. H. Wegdam, *Phys. Rev. Lett.* **1992**, *69*, 1975–1978.

[15] W. L. Miller, A. Cacciuto, *Phys. Rev. E* **2009**, *80*, 021404.

[16] H.-J. Butt, M. Kappl, *Adv. Colloid Interface Sci.* **2009**, *146*, 48–60.

[17] Q. Chen, S. C. Bae, S. Granick, *Nature* **2011**, *469*, 381–384.

[18] Q. Chen, J. Yan, J. Zhang, S. C. Bae, S. Granick, *Langmuir* **2012**, *28*, 13555–13561.

[19] a) M. E. Leunissen, R. Dreyfus, F. C. Cheong, D. G. Grier, R. Sha, N. C. Seeman, P. M. Chaikin, *Nat. Mater.* **2009**, *8*, 590–595; b) M. M. Maye, M. T. Kumara, D. Nykypanchuk, W. B. Sherman, O. Gang, *Nat. Nanotechnol.* **2010**, *5*, 116–120; c) F. Varrato, L. Di Michele, M. Belushkin, N. Dorsaz, S. H. Nathan, E. Eiser, G. Foffi, *Proc. Natl. Acad. Sci. USA* **2012**, *109*, 19155–19160.